GSA Data Repository 2017105; doi:10.1130/G38764.1

SUPPLEMENTAL METHODS

Grain size analysis

Two samples were taken from each push core (i) the 1 cm slice with the coarsest material and (ii) the 1 cm slice that visually appeared to contain the finest sediment. Grain-size analysis was conducted on a sub-sample of the 1 cm push core slices.

To ensure that the results of this study were directly comparable to those within Xu et al (2014), grain-size analysis was undertaken on the same Beckman Coulter LS230 laser diffraction particle size analyser, located at the USGS field office in Santa Cruz, California. Sample preparation also followed the same process used by Xu et al. (2014) and is outlined below.

Approximately 20 g of sediment was placed into individual 1000 mL beakers where 10 mL of 35% hydrogen peroxide (H_2O_2) was added along with sufficient distilled (DI) water to make a 300 mL solution. This solution was left overnight in order to remove organics and begin the process of sample dispersion. The following day, the samples were placed onto a hotplate set at 250-300 °C for 2-3 hours, or until the solution was concentrated to 200 mL: this ensured that any hydrogen peroxide was removed. Following this, each beaker was placed into an ultrasonic bath for 10 minutes to continue the disaggregation of fine mud particles.

The removal of soluble salts required two runs in a centrifuge. Samples were transferred into 250 ml centrifuge bottles. The bottles were weighed and in pairs, topped up with deionized water to within 0.1 g of each other. Each bottle within a pair was placed opposite each other within the centrifuge to ensure it was correctly balanced. Samples were centrifuged initially for 1 hour at 1700 rpm. After this initial run, samples were removed and the supernate removed without losing sample before samples were re-weighed while adding deionized water for a second 30 minute run at 1700 rpm. Following this, each sample had 5 ml of sodiumhexametaphosphate (calgon) added to disperse negatively charged clay particles. To ensure the weight of the calgon was accounted for, three aluminium trays were weighed before 5 mL of calgon was added and left to dry overnight in the oven.

Wet sieving was used to separate the sand and silt (2000-63 μm) fraction from the fines and mud fraction (<63 μm). Samples were washed: sand and silt sized grains were trapped in the sieve stack. Sand and silt were washed from the sieve and transferred into a crucible and then dried in an 80-110 °C oven overnight. Each graduated cylinder was topped up with deionized water to 1000 mL and left overnight.

The weight of each sample (both the dried sand and silt weight and the fines) was determined. The dry sand and silt were weighed and recorded. The dried weight of 20 mL of the fines solution was determined by drying the solution in an oven overnight and deducting the known weight of the calgon.

The Coulter counter was operated using the same protocol and parameters as described in Xu et al (2014). Approximately 1-2 g of sample was needed, with finer–grained samples requiring less sediment to achieve the correct obscuration. If the sample exceeded this 1-2 g guide, then it was split using a sand splitter before being added to the coulter chamber. Most samples were run using an obscuration of ~30%. It was necessary to run some samples with an obscuration as low as 4%. For the fine samples, the sample was transferred to a beaker and agitated using a motorised stirrer in order to achieve a homogeneous suspension. After two minutes of stirring a sample was taken using a pipette and added into the Coulter chamber. Each sample was passed through the counter three times, although the first run was discarded, because air bubbles were often present. The second and third runs were compared and if similar, then results were averaged. Between each run, the system was flushed to ensure no residual grains from the previous sample remained in the system. The coarse and fine samples, from a single grain-size sample (i.e. one push core slice), were combined using the bespoke USGS software, pc SDSZ, at the end of each run.

^{210}Pb dating

Sediment accumulation rates and ages were constrained by analysing for unsupported (excess) ^{210}Pb. ^{210}Pb is a naturally occurring radionuclide of the ^{238}U radioactive decay chain. Supported ^{210}Pb is derived from its parent radionuclide, ^{226}Ra ($t_{1/2}$ = 1600 years), within the sediment and is in secular equilibrium with its precursors in the ^{238}U decay series. In contrast, unsupported ^{210}Pb is formed by the decay of atmospheric ^{222}Rb ($t_{1/2}$ = 3.8 days) and accumulates in sediments through adsorption on suspended particulates (Swarzenski, 2014). ^{210}Pb has a half-life of 22.3 years and can therefore be used to establish sediment accumulation rates over the past 100 – 150 years.

The ^{210}Pb activity of samples was measured using gamma spectrometry at the USGS laboratories in Menlo Park, California. A 1 cm slice from the highest altitude push core (~70 m altitude) at each transect was used for the ^{210}Pb analysis. In the laboratory the samples where dried in an oven at 55°C over five days. The samples were weighed before and after drying to determine wet and dry sample weight, and sample porosity. Each dried sample was pulverized by hand using a ceramic mortal and pestle. The resulting powered-sediment was transferred to a scintillation vial and sealed, with the mass also noted.

1 or 2 centimeter intervals of sediment were counted in a calibrated high-purity Ge well-type gamma detector using the 46.52 keV (^{210}Pb), 351.87 and 609.31 keV (^{226}Ra) and the 661.6 keV (^{137}Cs) gamma energies. Precision in the activities of ^{210}Pb, ^{226}Ra, and ^{137}Cs were better than 5%. Excess ^{210}Pb derived geochronologies were calculated by deriving the inventories (I) of $^{210}Pb_{xs}$, ^{137}Cs, and ^{226}Ra using the following relationship:

$$I\ (dpm.cm^{-2}) = An \times M$$

where *M* is the cumulative mass (sum of mass depth in each layer) for each depth interval (g cm^{-2}), and *An* is the activity of each nuclide (i.e., $^{210}Pb_{xs}$, ^{137}Cs, or ^{226}Ra) per cumulative mass. The cumulative mass was calculated by adding the mass from each layer equivalent to the mass depth. Further details of these methods can be found in Swarzenski et al., 2006.

As several samples were taken at different depths within a core, sedimentation rates were calculated using a constant rate of supply method (Appleby and Oldfield, 1978), and is defined by:

$$C_d = C_0 e^{-kt}$$

Where C_d is the activity of ^{210}Pb at depth d, C_0 is the activity of ^{210}Pb at the core top (i.e. initial concentration of unsupported ^{210}Pb), k is the decay constant for ^{210}Pb (0.031), and t is the sedimentation rate. Least squares regression was used to establish the sedimentation rate of $Ln(^{210}Pb_{excess})$ as a function of depth.

SUPPLEMENTAL DISCUSSION

Flow thickness

We state that the three turbidity currents sourced in Monterey Canyon had a thin flow front that thickened through time. This conclusion is despite the final turbidity current not being captured at the shallowest mooring (R1) as a result of it breaking the mooring. We infer that the final turbidity current had a thin flow front because of the similarities in maximum velocities and thickness evolution between the three turbidity currents at deeper moorings. Additionally, the tilting and movement of the shallowest mooring by the second turbidity current happened during an initial high velocity phase of the turbidity current. It is not unreasonable to attribute the breaking of the mooring by the final turbidity current to a similar high velocity phase and thus a similar flow structure to previous turbidity currents.

SUPPLEMENTAL REFERENCES

Appleby, P.G., and Oldfield, F., 1978, The calculation of lead-210 dates assuming a constant rate of supply of unsupported ^{210}Pb to the sediment: Catena, v.5, p.1-8, doi:10.1016/S0341-8162(78)80002-2

Swarzenski, P. W., Baskaran, M., Rosenbauer, R. J., and Orem, W. H., 2006, Historical trace element distribution in sediments from the Mississippi River delta: Estuaries and Coasts, v. 29, p. 1094–1107, doi: 10.1007/BF02781812

Swarzenski, P. W. 2014, ^{210}Pb dating, *in* Rink, W.J., and Thompson, J., eds., Encyclopedia of Scientific Dating Methods,. Springer-Verlag, Berlin, p. 626-632, doi:10.1007/978-94-007-6326-5_236-1

SUPPLEMENTAL FIGURE AND TABLE CAPTIONS

Fig. DR1: Pressure, temperature, and schematic plots to highlight the translation and tilt of mooring R1 (original data presented in Xu et al., 2014). A) Pressure measurements at 170 (red) and 300 (blue) meters above seafloor. The increase in pressure signifies the onset of the turbidity current. The 20-minute measurement resolution of the pressure sensor means that the tilt is not record with these instruments (tilt lasts for ≤15 minutes) but the translation downslope, which occurs within 20-minutes, is highlighted by the pressure remaining at an elevated level. An ~18.4 dbar increase equates to ~18 m water depth increase. With an average slope of 1.8° and an 18 m depth increase, this equates to the mooring having travelled ~180 m down-canyon. B) Temperature plots at 170 (red) and 300 (blue) meters above seafloor. The temperature drop between 00 and 01 highlights the length and amount of mooring tilt. The 300 m temperature sensor drops to measure levels of the 170 m sensor indicates the amount of tilt on the mooring. The measurements are taken every five minutes. Three intervals during the temperature drop suggest the mooring was tilted for up to 15 minutes. The enlarged panels shows that the amount of tilt is the minimum amount of tilt. The mooring could have tilted more (dashed line) but not be recorded as the sensors only record every five minutes. C) Schematic representation of the mooring tilt. The 300 m sensors (blue) tilts to the level of the 170 m sensors (red). At the level of the sediment trap (70 meters), this tilt equates to 36.8 m depth increase. During this tilting the mooring is also translating down canyon.

Fig. DR2: Graphical logs and photos of three facies collected from Monterey Canyon. The *chaotic sand and gravel* could not be recovered as a complete core and is therefore not included.

Fig. DR3: Excess down-core ^{210}Pb ($xs^{210}Pb$) in disintegrations per minute (dpm). Each plot represents a different 70 m altitude core at a different transect (Tr1-6). Summary parameters of the linear regression (equation, r^2 value and sedimentation rate) are included on each plot.

Fig. DR4-DR9: Across canyon transects (looking down-canyon) at each transect location with each push core location and core photo. The different colors of the core photos may relate to different lighting of the photos or different cameras used. The contrast and brightness of the photos have been adjusted to highlight features.

Table DR1: Detailed push core locations including transect associations and altitude.

Table DR2: Detailed USGS mooring locations including water depth (Xu et al., 2004).

Table DR3: Characteristics of the four monitored turbidity currents (Xu et al., 2004; Xu 2010). Flow thicknesses were calculated from the ADCP velocity profiles (for methods see Xu, 2010).


A
Pressure dbar
30
20
10
0
16
17
18
19
20
21
22
23
24
25
Dec 19 2002
Translation downslope
(~18 dbar = 18.4 m)
300 meters altitude
170 meters altitude
B
Temperature (˚C)
6.5
6
5.5
5
16 17 18 19 20 21 22 23 00 01 02 03 04 05 06 07 08 09 10 11 12 13
Dec 19 2002
300 meters altitude
170 meters altitude
C
Pressure and temperature sensors: 300 meters altitude
Pressure and temperature sensors: 170 meters altitude
Based on the temperature data, the 300 m altitude temperature sensor (blue) dips down to the level of the 170 m altitude sensor (red). This tilt lasts for a maximum of 15 minutes.
Sediment trap: 70 meters altitude
36.8 m
The sediment trap dipped enough to be within the body of the flow. This is thought to be the minimum amount of tilt (see zoomed section of B above)
Seafloor
The mooring translates ~580 m downslope at ~0.5 m/s

Fig. DR1

Fig. DR2

A. Clean sands
B. Interbedded sands and silty mud
C. Silty mud
Grain size (μm)
64
125
250
375
Depth (cm)
0
5
10
15
20
Sand
Mud
Bioturbation - burrow

Fig. DR3

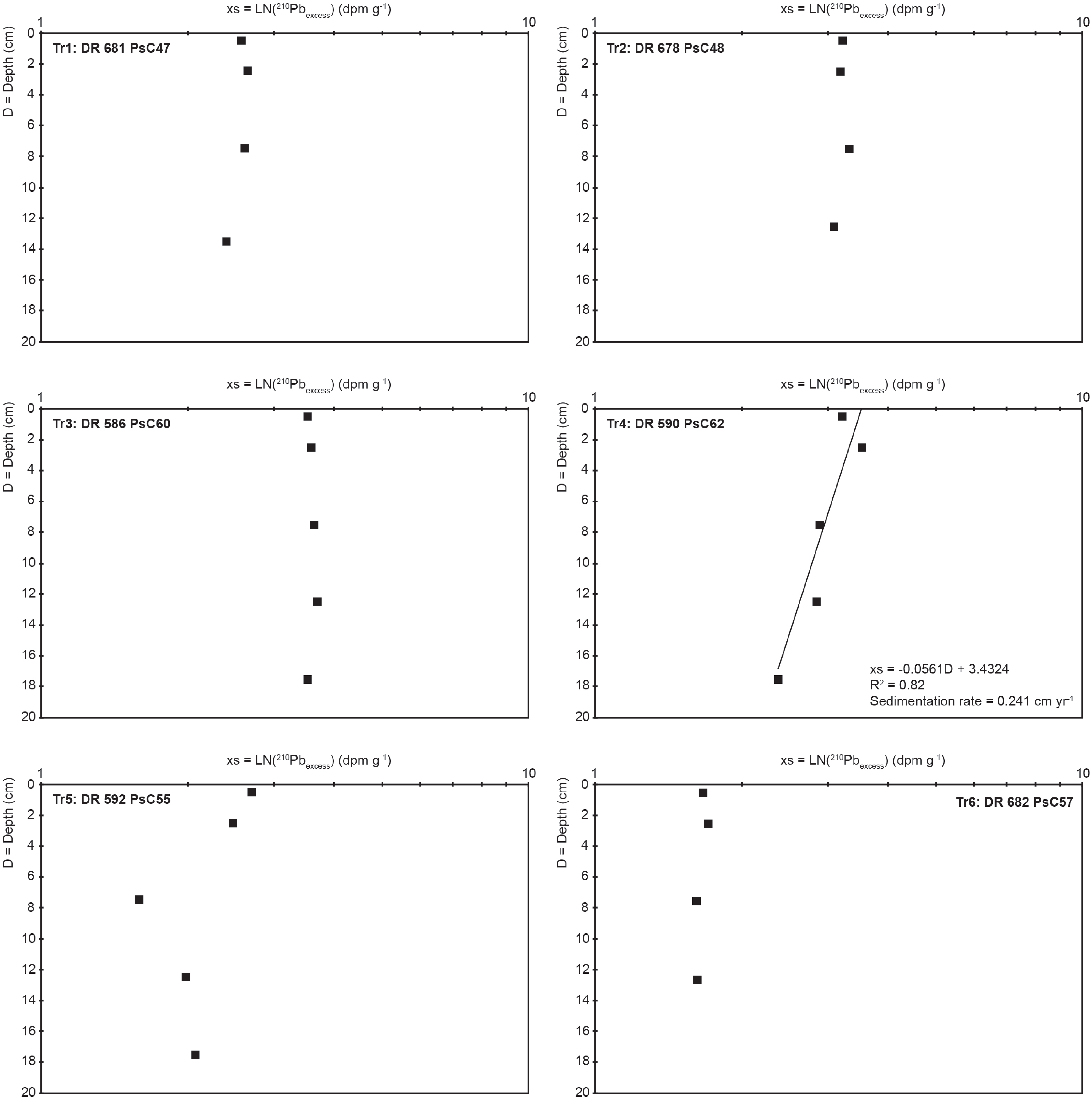
xs = LN($^{210}Pb_{excess}$) (dpm g^{-1})
D = Depth (cm)
Tr1: DR 681 PsC47
Tr2: DR 678 PsC48
Tr3: DR 586 PsC60
Tr4: DR 590 PsC62
xs = -0.0561D + 3.4324
R^2 = 0.82
Sedimentation rate = 0.241 cm yr^{-1}
Tr5: DR 592 PsC55
Tr6: DR 682 PsC57


F. DR681 PsC51
Silty mud
D. DR681 PsC51
Silty mud
E. DR681 PsC46
Silty mud
A. DR681 PsC76
Silty mud
B. DR681 PsC64
Indurated substrate
C. DR681 PsC45
Silty mud
F. DR681 PsC58
Indurated substrate
D. DR681 PsC60
Indurated substrate
E. DR681 PsC72
Indurated substrate
A. DR681 PsC43
Indurated substrate
B. DR681 PsC79
Indurated substrate
C. DR681 PsC63
Indurated substrate
Depth (cm)
Water Depth (m)
Distance (m)
A
B
C
D
E
F
0
200
400
600
800
220
240
260
280
300

Fig. DR4

Fig. DR5

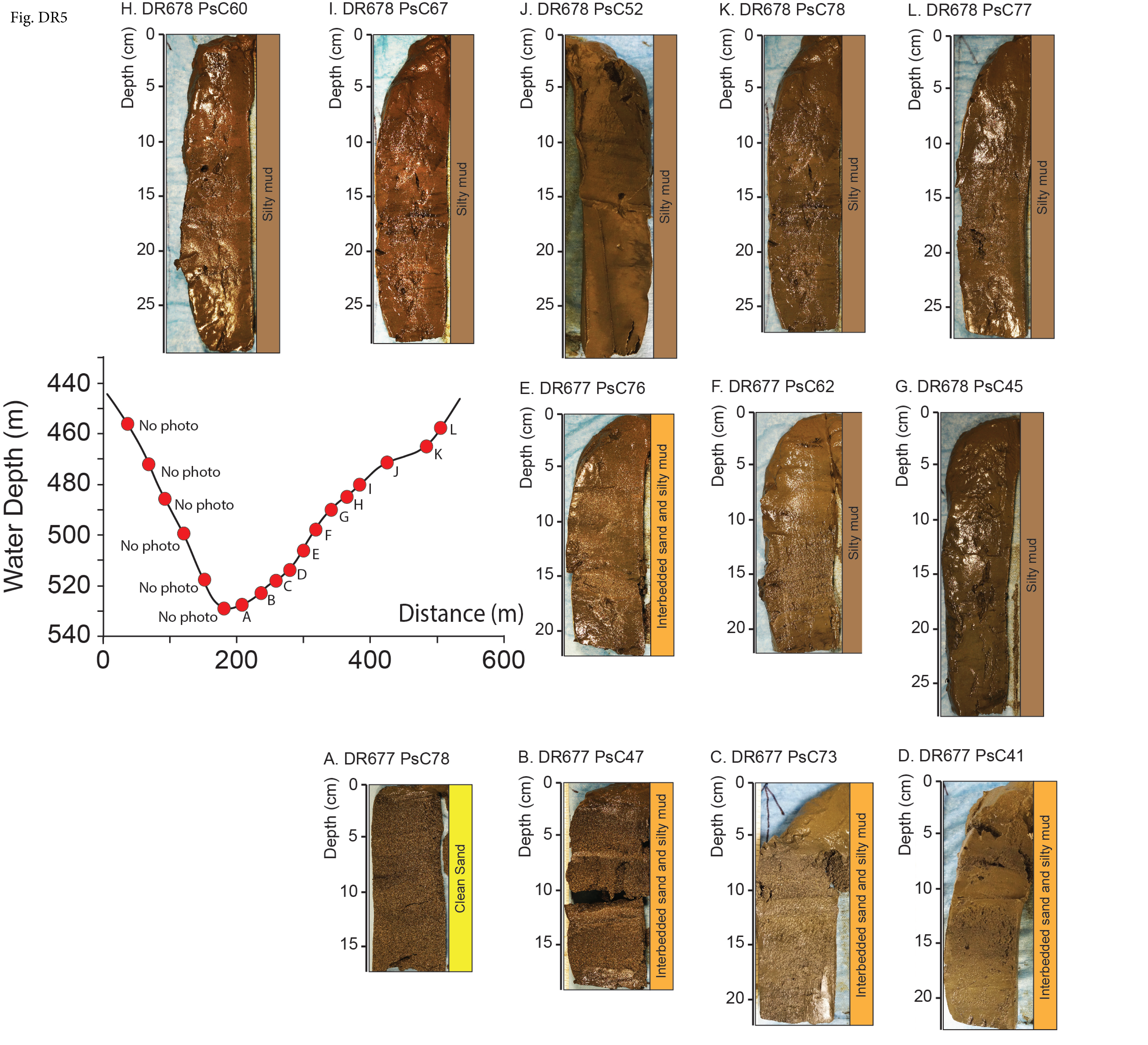
H. DR678 PsC60
I. DR678 PsC67
J. DR678 PsC52
K. DR678 PsC78
L. DR678 PsC77
Depth (cm)
Silty mud
Water Depth (m)
Distance (m)
No photo
E. DR677 PsC76
F. DR677 PsC62
G. DR678 PsC45
Interbedded sand and silty mud
A. DR677 PsC78
B. DR677 PsC47
C. DR677 PsC73
D. DR677 PsC41
Clean Sand


G. DR685 PsC70
Indurated substrate
H. DR685 PsC54
Indurated substrate
I. DR685 PsC63
Indurated substrate
J. DR685 PsC74
Indurated substrate
H. DR586 PsC43
Silty mud
I. DR586 PsC48
Silty mud
J. DR586 PsC51
Silty mud
K. DR586 PsC66
Silty mud
E. DR680 PsC58
Silty mud
F. DR680 PsC50
Indurated substrate
F. DR585 PsC45
Interbedded sand and silty mud
G. DR586 PsC72
Interbedded sand and silty mud
A. DR685 PsC62
Clean Sand
B. DR685 PsC42
Interbedded sand and silty mud
C. DR680 PsC47
Interbedded sand and silty mud
D. DR680 PsC46
Silty mud
B. DR585 PsC66
Clean Sand
D. DR585 PsC61
Interbedded sand and silty mud
E. DR585 PsC52
Interbedded sand and silty mud
Depth (cm)
Water Depth (m)
Distance (m)
L - No photo
C - No photo
A - No photo

Fig. DR6

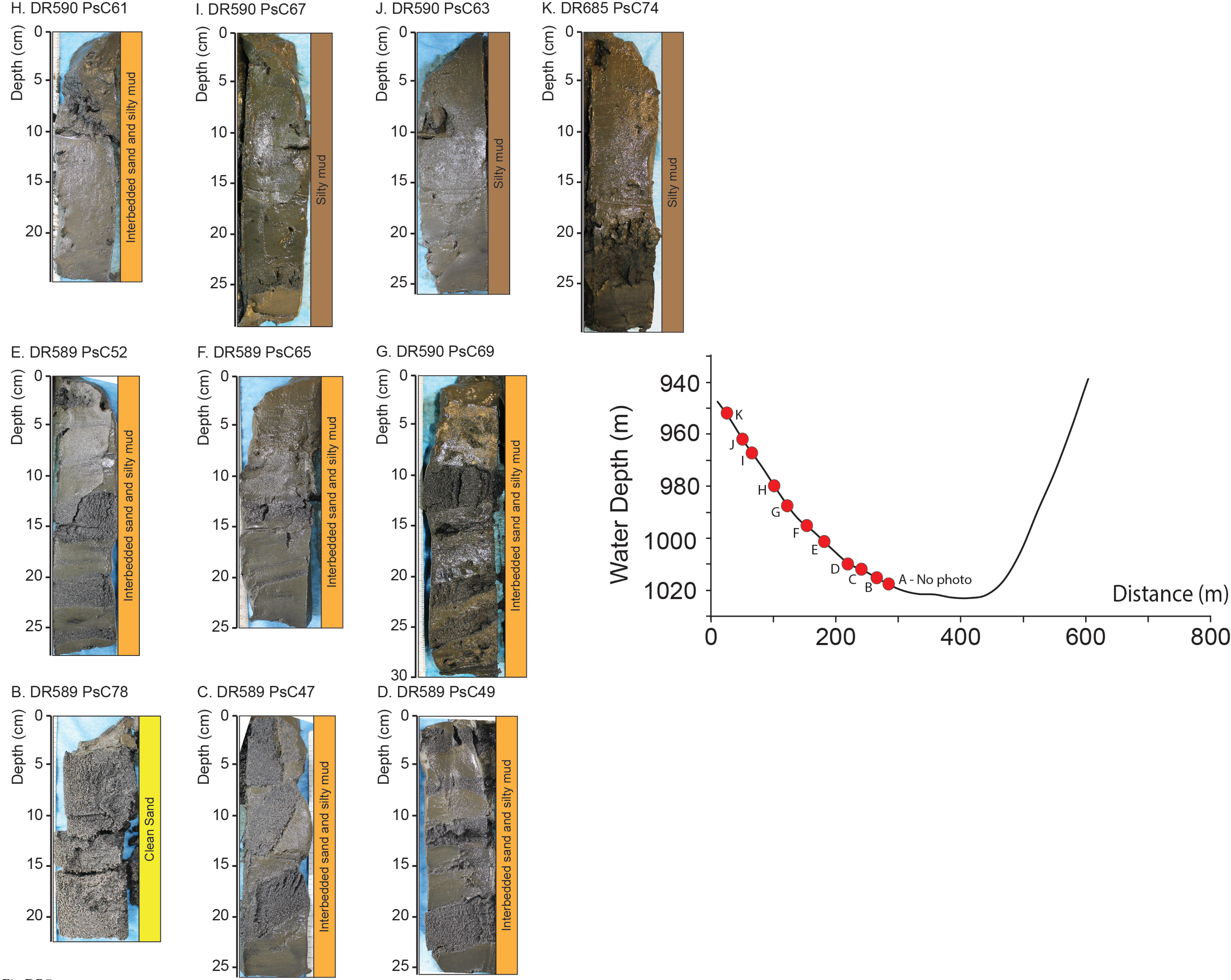

H. DR590 PsC61
Depth (cm)
Interbedded sand and silty mud
I. DR590 PsC67
Depth (cm)
Silty mud
J. DR590 PsC63
Depth (cm)
Silty mud
K. DR685 PsC74
Depth (cm)
Silty mud
E. DR589 PsC52
Depth (cm)
Interbedded sand and silty mud
F. DR589 PsC65
Depth (cm)
Interbedded sand and silty mud
G. DR590 PsC69
Depth (cm)
Interbedded sand and silty mud
B. DR589 PsC78
Depth (cm)
Clean Sand
C. DR589 PsC47
Depth (cm)
Interbedded sand and silty mud
D. DR589 PsC49
Depth (cm)
Interbedded sand and silty mud
Water Depth (m)
940
960
980
1000
1020
Distance (m)
0
200
400
600
800
K
J
I
H
G
F
E
D
C
B
A - No photo

Fig DR7


H. DR592 PsC69
I. DR592 PsC77
J. DR592 PsC64
K. DR592 PsC66
L. DR592 PsC62
E. DR591 PsC49
F. DR591 PsC64
G. DR592 PsC71
A. DR591 PsC77
B. DR591 PsC76
C. DR591 PsC57
D. DR591 PsC74
Depth (cm)
Interbedded sand and silty mud
Silty mud
Water Depth (m)
Distance (m)
1200
1220
1240
1260
1280
1300
1320
1340
0
200
400
600
800
1000
1200
L
K
J
I
H
G
F
E
D
C
B
A

Fig. DR8

Fig. DR9

Water Depth (m)
1440
1460
1480
1500
1520
1540
Distance (m)
0
200
400
600
A
B
C
D
E
F
G
H
I
J
K
L
I. DR682 PsC70
J. DR682 PsC50
K. DR682 PsC63
L. DR682 PsC77
E. DR679 PsC41
F. DR679 PsC77
G. DR682 PsC67
H. DR682 PsC42
A. DR679 PsC69
B. DR679 PsC67
C. DR679 PsC45
D. DR679 PsC72
Depth (cm)
0
5
10
15
20
25
Silty mud
Interbedded sand and silty mud

Table DR1: Detailed push core locations including transect associations and altitude.

Transect	Core number	Altitude (m)	Latitude	Longitude
Tr1 north wall	DR681 PsC 53	0.03	36.794487	121.844739
	DR681 PsC 42	27.76	36.794934	121.844696
	DR681 PsC 54	36.59	36.795153	121.844639
	DR681 PsC 67	44.56	36.795684	121.844428
	DR681 PsC 57	53.26	36.796102	121.844332
	DR681 PsC 70	57.1	36.797717	121.843964
Tr1 south wall	DR683 PsC 57	0.01	36.792304	121.845408
	DR683 PsC 63	6.85	36.792202	121.845399
	DR683 PsC 58	30.59	36.791763	121.845488
	DR683 PsC 75	41.3	36.791545	121.845518
	DR683 PsC 42	51.15	36.791294	121.845608
	DR683 PsC 52	62.19	36.79068	121.845698
Tr2 north wall	DR677 PsC 78	0.01	36.788592	121.902991
	DR677 PsC 54	7.76	36.788581	121.903618
	DR677 PsC 43	17.07	36.788658	121.904332
	DR677 PsC 70	30.77	36.788602	121.904764
	DR678 PsC 43	46.14	36.788549	121.90533
	DR678 PsC 78	59.45	36.788628	121.906063
	DR678 PsC 72	71.98	36.788588	121.907336
Tr2 south wall	DR687 PsC 58	0	36.788719	121.9029
	DR687 PsC 47	13.05	36.788624	121.902603
	DR687 PsC 64	30.99	36.788799	121.902321
	DR687 PsC 74	44.32	36.788723	121.901854
	DR687 PsC 56	59.2	36.788789	121.901603
	DR687 PsC 45	72.91	36.788781	121.901226
Tr3 north wall	DR585 PsC 64	1.37	36.76513	121.969405
	DR585 PsC 79	7.74	36.765919	121.969977
	DR585 PsC 74	21.91	36.766338	121.970698
	DR586 PsC 56	35.07	36.767173	121.971071
	DR586 PsC 67	56.76	36.767823	121.971461
	DR586 PsC 60	74.93	36.768652	121.971543
Tr3 south wall	DR685 PsC 49	0.01	36.764466	121.968944
	DR685 PsC 64	8.2	36.764101	121.968603
	DR680 PsC 47	11.68	36.764026	121.968444
	DR680 PsC 64	28.96	36.763797	121.96822
	DR685 PsC 77	49.44	36.763424	121.967913
	DR685 PsC 51	70.26	36.763126	121.967586
	DR685 PsC 80	78.38	36.762994	121.967471

Tr4 north wall	DR589 PsC 77	2	36.781507	122.016136
	DR589 PsC 75	4.36	36.781083	122.016472
	DR589 PsC 71	15.51	36.780547	122.016652
	DR590 PsC 75	28.67	36.779837	122.017104
	DR590 PsC 51	36.59	36.779565	122.017242
	DR590 PsC 52	48.64	36.779321	122.017397
	DR590 PsC 62	64.44	36.77891	122.017268
Tr5 south wall	DR591 PsC 47	9.83	36.734525	122.013342
	DR591 PsC 43	13.32	36.734721	122.013248
	DR591 PsC 75	0.41	36.734157	122.014367
	DR592 PsC 56	38.7	36.735102	122.012422
	DR592 PsC 44	53.58	36.735316	122.01206
	DR592 PsC 55	71.81	36.735545	122.01179
Tr6 north wall	DR679 PsC 64	0	36.702313	122.02049
	DR679 PsC 79	5.33	36.702505	122.020895
	DR679 PsC 63	11.49	36.702728	122.021185
	DR679 PsC 76	21.37	36.703056	122.021483
	DR682 PsC 76	44.09	36.703305	122.021926
	DR682 PsC 46	58.08	36.703521	122.022221
	DR682 PsC 41	74.55	36.703783	122.022662

Table DR2: Detailed USGS mooring locations including water depth (Xu et al., 2004).

Mooring	Water depth	Latitude	Longitude
R1	820	36.77167	121.9632
R2	1020	36.78033	122.0135
R3	1445	36.7195	122.0125

Table DR3: Characteristics of the four monitored turbidity currents (Xu et al., 2004; Xu 2010). Flow thicknesses were calculated from the ADCP velocity profiles (for methods see Xu, 2010).

Turbidity Current	Date	Source	Trigger	Mooring R1				Mooring R2				Mooring R3			
				Thickness		Max speed	Max speed	Thickness		Max speed	Max speed	Thickness		Max speed	Max speed
				Time (hr)	Thickness (m)*	(cm/s)	elevation (m)	Time (hr)	Thickness (m)	(cm/s)	elevation (m)	Time (hr)	Thickness (m)	(cm/s)	elevation (m)
TC1	17-Dec-02	Soquel canyon	Storm activity that possibly caused failure of Soquel canyon wall or floor.					1	30.2	60	12.5	4	57.1	75	9.3
					Not recorded at mooring as Soquel tributary intersects Monterey downstream of R1			2	24.2			5	50.2		
								3	34.6			6	48.2		
								4	39.7			7	54.7		
								5	27.2			8	39.8		
												9	26.7		
TC2	20-Dec-02	Monterey Canyon	Storm activity transported large amounts of sediment to the canyon head which failed under wave loading.	1	23.9	190	12.2	1	37.5	160	10.5	2	31.1	180	5.3
				2	33			2	38.2			3	55.6		
				3	35.1			3	43.2			4	58.1		
				4	34.1			4	48.5			5	52.5		
				5	29.2			5	51.3			6	55.1		
				6	28.2			6	33.1			7	53.5		
				7	51.4							8	53.5		
				8	55.5							9	37		
												10	25.8		
TC3	14-Mar-03	Monterey Canyon	Anthropogenic. Dredged material dumped at the head of Monterey Canyon	1	32.4	160	12.2	2	32.2	105	8.5				
				2	33.6			3	32.3						
				3	39.9			4	42.5				*Turbidity current did not reach mooring*		
				4	38.2			5	45.9						
				5	45.6			6	47.7						
				6	53.7										
TC4	19-Nov-03	Monterey Canyon	Unknown					1	41.8	155	10.5	3	46.3	110	7.3
								2	46.5			4	56		
								3	49.7			5	58		
					Turbidity current broke mooring			4	51.9			6	58.5		
								5	52.4						
								6	52.9						
								7	49.3						